Single-Molecule Studies

International Edition: DOI: 10.1002/anie.201813888
German Edition: DOI: 10.1002/ange.201813888

Detecting Single-Molecule Dynamics on Lipid Membranes with Quenchers-in-a-Liposome FRET

Dong-Fei Ma, Chun-Hua Xu, Wen-Qing Hou, Chun-Yu Zhao, Jian-Bing Ma, Xing-Yuan Huang, Qi Jia, Lu Ma, Jiajie Diao, Cong Liu, Ming Li,* and Ying Lu**

Abstract: *Tracking membrane-interacting molecules and visualizing their conformational dynamics are key to understanding their functions. It is, however, challenging to accurately probe the positions of a molecule relative to a membrane. Herein, a single-molecule method, termed LipoFRET, is reported to assess interplay between molecules and liposomes. It takes advantage of FRET between a single fluorophore attached to a biomolecule and many quenchers in a liposome. This method was used to characterize interactions between α-synuclein (α-syn) and membranes. These results revealed that the N-terminus of α-syn inserts into the membrane and spontaneously transitions between different depths. In contrast, the C-terminal tail of α-syn is regulated by calcium ions and floats in solution in two conformations. LipoFRET is a powerful tool to investigate membrane-interacting biomolecules with sub-nanometer precision at the single-molecule level.*

Liposomes are widely used as models for studying protein–membrane interactions and for elucidating binding mechanisms of drugs and antibiotics on target cells.[1] In these aspects, information about the positional changes of a site of interest in the direction normal to the membrane (*z* direction) is more important than parallel to the membrane (*xy* directions) because the membranes are fluidic. Applications of time- and ensemble-averaging techniques to these model systems have resulted in valuable data.[2] It is still challenging to gain information about positional changes and structural dynamics of a single membrane-interacting molecule relative to the liposome surface, though a few techniques have been reported to yield some information using solid-supported lipid bilayers.[3] Single-molecule fluorescent resonance energy transfer (smFRET) can probe nanoscale movements of fluorophore-labeled proteins on liposome surfaces,[2c,4] but the point-to-point energy transfer of smFRET makes it difficult to distinguish motions in the *z* direction from those in the *xy* directions. Herein, we developed a single-molecule method that we term LipoFRET to resolve this challenge. We validated the method by positioning fluorophores at different regions relative to the membrane surface, and then applied the method to characterize the membrane binding activity of α-synuclein (α-syn), a key player in the pathology of Parkinson's disease and presynaptic vesicle homeostasis.[5] Our approach yielded quantitative information about the positions of different regions of α-syn in lipid bilayers at the single-molecule level.

This method is based on FRET between a fluorophore and a multitude of quenchers encapsulated in a liposome (Figure 1 a), hence the name LipoFRET. The energy transfer

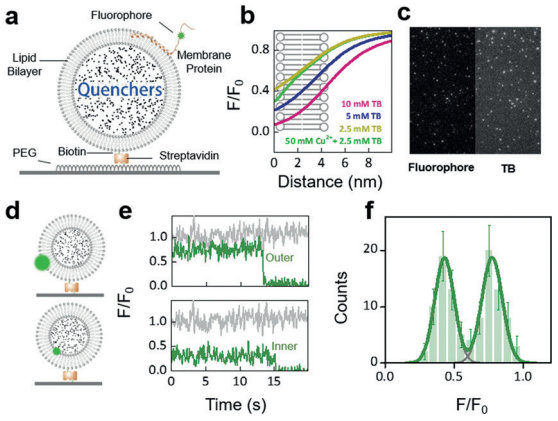

Figure 1. Principle of LipoFRET. a) A fluorophore around a liposome full of quenchers. b) Calculated quenching efficiency against distance for various quencher concentrations used to convert fluorescence intensity into distance. c) Typical images of fluorophores (α-syn T72C–Alexa555) and liposomes containing TB for the co-localization analysis. d) Fluorophores on the outer surface (upper panel) and the inner surface of the liposomes (lower panel). e) The green traces correspond to fluorophores on the outer surface (upper panel) and the inner surface of the liposomes (lower panel). The trace for liposome without quenchers (gray lines) is also displayed for comparison. f) Histograms of the relative fluorescent intensities. Error bars on the histograms represent the statistical error in the bins. The statistics are from 105 traces.

[*] D.-F. Ma, C.-H. Xu, W.-Q. Hou, J.-B. Ma, X.-Y. Huang, Q. Jia, L. Ma, M. Li, Y. Lu
Beijing National Laboratory for Condensed Matter Physics and CAS Key Laboratory of Soft Matter Physics, Institute of Physics, Chinese Academy of Sciences, Beijing 100190 (China)
E-mail: mingli@iphy.ac.cn
yinglu@iphy.ac.cn

C.-Y. Zhao, C. Liu
Interdisciplinary Research Center on Biology and Chemistry, Shanghai Institute of Organic Chemistry, Chinese Academy of Sciences, Shanghai 200032 (China)
E-mail: liulab@sioc.ac.cn

D.-F. Ma, C.-H. Xu, W.-Q. Hou, C.-Y. Zhao, J.-B. Ma, X.-Y. Huang, Q. Jia, L. Ma, C. Liu, M. Li, Y. Lu
University of Chinese Academy of Sciences, Beijing 100049 (China)

J. Diao
Department of Cancer Biology, University of Cincinnati School of Medicine, Cincinnati, OH 45267 (USA)

M. Li, Y. Lu
Songshan Lake Materials Laboratory
Dongguan, Guangdong 523808 (China)

Supporting information and the ORCID identification number(s) for the author(s) of this article can be found under: https://doi.org/10.1002/anie.201813888.

kinetics k_t is the sum of pairwise transfer rates k_{ti} (see Figure S1 in the Supporting Information),[6]

$$k_t = \sum_{i=1}^{N} k_{ti} = \frac{1}{\tau}\sum_{i=1}^{N}\left(\frac{r_{0i}}{r_i}\right)^6, \quad (1)$$

where τ refers to the intrinsic lifetime of the donor, and r_{0i} and r_i are the Förster distance and the spatial distance between the i^{th} donor–acceptor pair, respectively. The energy-transfer efficiency is given by $E = k_t/(\tau^{-1} + k_t)$, which is used to calculate the relative fluorescence of the donor, $F/F_0 = 1-E$, where F_0 is the intrinsic fluorescence without the quenchers.

Because the mean inter-quencher distance is comparable to the Förster distance r_0 in our experiments, the quencher solution cannot be treated as a continuous medium. We therefore performed Monte Carlo simulation to calculate the ensemble average of k_t in Equation (1) (details are in the Supporting Information), taking into account the fact that the measured efficiency is an average over the exposure time of the CCD camera, which is much longer than the lifetime of the fluorophore. The curves in Figure 1 b illustrate a few examples resulting from the calculations. Such curves were used to convert measured F/F_0 to distance with respect to the inner surface (see the supplementary text in the Supporting Information).[3b] F/F_0 increased steeply as the fluorophore moved from the inner surface to outside the liposome. The region of sensitivity shifted from around the inner bilayer to around the outer surface as the concentration of quenchers increased from 2.5 to 10 mM. This shifting is of importance for practical applications because the region of sensitivity of LipoFRET is usually only a few nanometers. If necessary, one may add some quenchers with short Förster distances[7] to attenuate the fluorophore only near the inner surface to enhance the sensitivity there (dark yellow and green lines in Figure 1 b).

The fluorescence of both the donor and the liposome was measured in a standard two-channel FRET setup following a co-localization protocol[8] to make sure that the quenching is indeed due to the quenchers in the liposome (Figure 1 c and Supporting Information, Figures S1c and S2). Only donors that could be co-localized with the liposomes were analyzed. Many dyes,[9] and even metal ions, can be used as quenchers as long as their absorption spectra have some overlap with the emission spectrum of the donor. The fluorescence of the quenchers should be weak enough so that the emission from the liposome does not interfere with the donor. In the current work, we chose trypan blue (TB) and Cu^{2+}-nitrilotriacetic acid complex (Cu–NTA) as quenchers (spectrums in Figure S8 in the Supporting Information). TB is widely used in dye exclusion assays[10] and flow cytometry analysis.[11] The biological applications suggest that TB is a low-cytotoxicity dye[12] that is not likely to damage the liposomes. Though TB alone was good enough for LipoFRET to detect dynamics in some regions around the membrane, we can add Cu–NTA to further increase the sensitivity near the inner surface of the liposome (green line in Figure 1 b). Cu–NTA was previously used in a transition-metal ion FRET approach to probe the configuration dynamics of proteins.[7]

The feasibility of LipoFRET was demonstrated by measuring the quenching efficiency of fluorophores conjugated to lipid headgroups. Unilamellar liposomes were prepared and immobilized onto a streptavidin-modified glass surface via 16:0 biotinyl-capped phosphatidylethanolamine (PE, Biotin–PE). The liposomes were doped with Alexa Fluor 555-labeled PE (PE–Alexa555) with 0.001 % molar fraction. The low molar ratio ensures that a majority of the liposomes contain one or zero fluorophores (see the supplementary text in the Supporting Information for more details).[13] The intrinsic fluorescence F_0 of PE–Alexa555 was measured on liposomes containing PBS buffer (Supporting Information, Figure S4). For liposomes containing 2.5 mM TB, the fluorescence of PE-Alexa555 was significantly attenuated, as predicted by our calculations (dark yellow line in Figure 1 b). Two relative intensities ($F/F_0 = 0.42 \pm 0.08$ and 0.77 ± 0.09 (mean ± s.d.)) were observed, representing the fluorophores on the inner and outer surfaces, respectively (Figure 1). The centers of the two peaks in Figure 1 e correspond to a separation of 4.5 ± 1.1 (mean ± s.d.) nm, consistent with the thickness of the lipid bilayer,[14] indicating that LipoFRET is precise enough to measure the location of a single fluorophore in the lipid bilayer.

Membrane-interacting biomolecules are usually not completely embedded in bilayers.[15] So far, no well-established technique is able to accurately detect the positional changes of single biomolecules in proximity to liposome membranes. An experiment was designed to show the capability of LipoFRET in this aspect. Single-stranded DNA (ssDNA) of 10-nucleotides in length was anchored to DOPC liposomes in which 5 mM TB was encapsulated. The two ends of the ssDNA segment were labeled with tetramethylrhodamine (TAMRA) and cholesterol, respectively. The hydrophobic CH moieties could spontaneously incorporate into the lipid bilayer thus anchoring the DNA on the membrane.[16] The relative fluorescence F/F_0 of TAMRA was centered at 0.71 ± 0.06, suggesting that the fluorophore was only 1.3 ± 0.6 nm above the liposome outer surface. The fluorescence intensity of TAMRA labeling a double-stranded DNA (dsDNA) of 10-nucleotides in length was then measured. The F/F_0 was 0.86 ± 0.07, corresponding to a height of 3.3 ± 1.1 nm above the outer surface of the liposome (Figure 2). The results are in accordance with the expectation that the floppy ssDNA is in

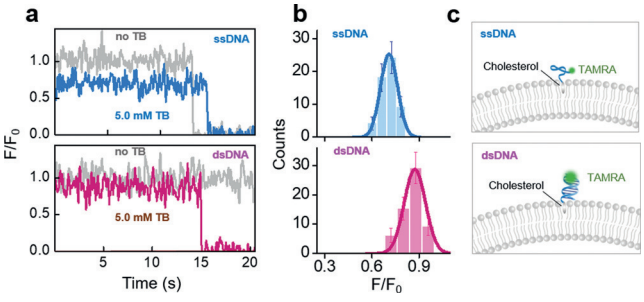

Figure 2. ssDNA and dsDNA on liposomes. a) Typical traces of TAMRA-labeled ssDNA (blue) and dsDNA (red) anchored on the liposome with 5 mM TB. b) Intensity histograms of the fluorophores for ssDNA (blue) and dsDNA (red). More than 50 traces were used to build the histograms. Error bars on the histograms represent the statistical error in the bins. c) Configurations of ssDNA and dsDNA on liposomes.

close proximity to the liposome surface, while the rigid dsDNA stands upright on the surface.[17] We also applied LipoFRET to the LL-37 peptide and obtained similar results as in our previous work on solid-supported lipid bilayers[3a] (Supporting Information, Figure S5), further demonstrating the validation of LipoFRET.

The dynamic interplay between α-syn and the membrane is believed to be important in mediating the function of α-syn in synaptic vesicle trafficking and pathological aggregation.[18] However, the function of α-syn is largely unknown, and its conformation in the membrane is still in debate.[2a,b,19] Liposomes composed of DOPC/DOPA (7:3) were prepared and Alexa555-labeled α-syn in PBS buffer (pH 7.4, 150 mM NaCl) was used as the donor. As representatives, we selected three sites in α-syn to depict the general pattern of the protein on the liposome, which were S129 that locates in the C-terminal flexible acidic tail, T72 in the central alpha-helix, and K10 at the N-terminus. The relative fluorescence of T72C–Alexa555 was $F/F_0 = 0.64 \pm 0.07$, while that of S129C-Alexa555 was 0.87 ± 0.07 (Figure 3a,b). The intensity of T72C-Alexa555 is consistent with our calculation (Figure 1b), assuming that α-syn adopts a helical conformation with T72 being on the hydrophilic side of the alpha-helix[2b] (Figure 3a). For the site S129, the high fluorescent intensity in Figure 3b indicates that this site was 2.9 ± 1.5 nm higher than T72 above the outer surface of the liposome.

The interaction of the N-terminus of α-syn with the lipid bilayer has been intensively investigated.[20] Some researchers reported that this region is fully buried in the acyl chains by using neutron reflectivity and bromine quenching,[20a,b] but others showed that the whole helix stays on the surface.[20c] In our measurements, liposomes containing 2.5 mM TB plus 50 mM Cu–NTA were used to enhance the sensitivity in the deep region of the membrane. The fluorescence of K10C–Alexa555 transitioned slowly between multiple values on a timescale of a few seconds (Figure 3c and Supporting Information, Figures S6 and S7). Although a few traces exhibited more than three states, only three main peaks could be clearly identified in the histogram because of the low frequency occurrences of some states and the limited resolution. The highest relative intensity was $F/F_0 = 0.84 \pm 0.06$ and was located on the outer surface of the lipid bilayer. The medium intensity, $F/F_0 = 0.68 \pm 0.07$, was 1.2 ± 0.7 nm below the outer surface. The lowest intensity was $F/F_0 = 0.44 \pm 0.07$, suggesting that the position was about 3.4 ± 0.5 nm below the outer surface. To our knowledge, this is the first quantitative data regarding the dynamics of the N-terminus of α-syn in lipid membranes. Time- and ensemble-averaging techniques, such as neutron reflectivity and tryptophan fluorescence quenching by bromine, showed that α-syn penetrates the membrane by 1-1.5 nm.[20a,b] We believe that those values were just the average of the different depths observed here.

The C-terminal tail of α-syn is likely involved in Ca^{2+} binding because α-syn is implicated to function in dopamine and Ca^{2+} signaling.[21] Effects of Ca^{2+} reported in the literature are controversial. Some showed that Ca^{2+} binds to the C-terminus of α-syn and triggers a conformational change and interaction of the C-terminus with lipid bilayers.[22] But other research showed that Ca^{2+} binds to the anionic lipids and weakens the α-syn membrane interaction.[23] We examined the effect of Ca^{2+} on the acidic tail of the liposome-bound α-syn in 10 mM HEPES buffer (pH 7.4, 10 mM NaCl). When Ca^{2+} was added, two intensities were observed for S129C–Alexa555 (Figure 4), which correspond to two states

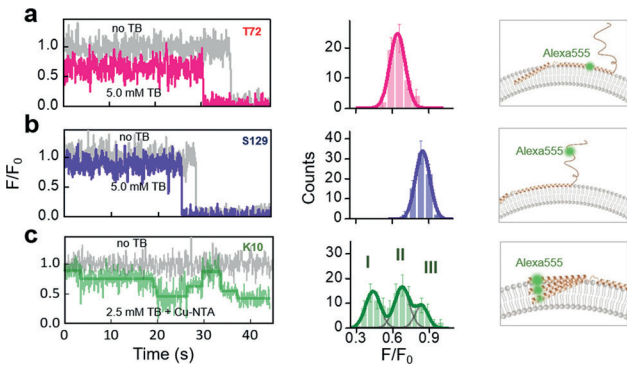

Figure 3. Positions of three sites of interest in α-syn. a) Typical fluorescent traces, intensity histogram, and scheme of α-syn labeled at T72 on a liposome. b) Results for the site S129. More than 60 traces were used to build the histograms. c) The site K10 of α-syn transitions between three penetration depths. The statistics were from 120 states. Error bars on the histograms represent the statistical error in the bins.

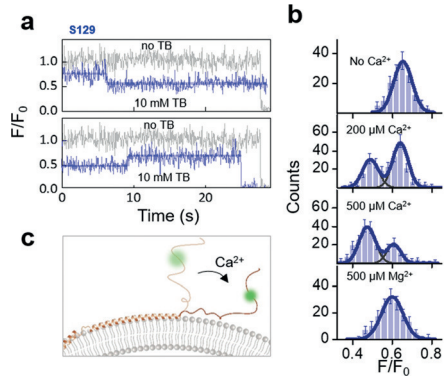

Figure 4. Calcium regulation of the α-syn C-terminal tail. a) Typical traces. b) The intensity histograms of S129–Alexa555 in various concentrations of Ca^{2+} (0 to 500 μM) are compared with that in the presence of 500 μM Mg^{2+}. c) Scheme of α-syn labeled at S129 without or with Ca^{2+}. The statistics are from 141, 242, 227, and 229 traces at different concentrations of Ca^{2+}, respectively.

with and without a Ca^{2+} bound, respectively. The population of low fluorescence was smaller than that of high fluorescence at 200 μM Ca^{2+}. The ratio was reversed at 500 μM Ca^{2+}. The results are consistent with the previous observation that the half-saturation concentration of Ca^{2+} binding to α-syn is about 300 μM.[21a] In a control experiment with 500 μM Mg^{2+}, only one intensity was observed, which was almost equal to the high-fluorescence intensity in the experiments with Ca^{2+}. The shift of the high-fluorescence peak to lower intensity in Figure 4b resulted from the non-specific Coulomb screening of the C-terminal tail by Ca^{2+}. The same screening also

manifested in the control experiment with Mg^{2+} (bottom panel in Figure 4b). Because of the Coulomb screening effect, the difference in height between the two states was 1.6 ± 0.9 nm at 200 μM Ca^{2+} and 1.2 ± 0.9 nm at 500 μM Ca^{2+}. Since Ca^{2+} ions reduced the height of S129 to a much smaller value (Figure 4c), we speculate a specific interaction between the C-terminal tail and Ca^{2+}. To our knowledge, the distance between the membrane surface and any residues in the C-terminal tail of α-syn has not been accurately measured before, although it has long been proposed that the negatively charged acidic tail (residues 96–140) flaps in solution when the N-terminus anchors onto a negatively charged lipid bilayer.[2a,20b]

Probing the structural dynamics of proteins at lipid membranes has been a very difficult task. We demonstrated the feasibility of LipoFRET in quantitating the positional changes of a site of interest in the membrane-interacting protein not only inside but also outside the lipid membrane. Both are crucial to understanding protein–membrane and protein–ligand interactions. The interplay of α-syn with membranes has long been a subject of debate. The existence of multiple states of α-syn in the membrane may explain why different results were reported in the literature. The homogenous aqueous environment around the unstructured tail poses an obstacle to almost any environment-dependent methods to determine its position above the membrane. LipoFRET is not subject to this limitation, and therefore is suitable for the detailed characterization at the single-molecule level in this case. Extending LipoFRET to other applications is straightforward. For example, phospholipid flip-flops in membranes are involved in many physiological processes, such as cell apoptosis.[24] LipoFRET may also be used to monitor the translocation of a fluorophore-labeled indicator through a transporter.[25] LipoFRET is easy to implement and does not require complicated instrumentation. We anticipate that LipoFRET will have widespread applications in the study of membrane systems.

Acknowledgements

This work was supported by the National Science Foundation of China (Grants No. 11674382, No. 11834018, No. 91753104 and No. 11574381) and by the CAS Key Research Program of Frontier Sciences (Grant No. QYZDJ-SSW-SYS014). Y.L. is supported by the Youth Innovation Promotion Association of CAS (No. 2017015). The authors gratefully acknowledge the support of the K. C. Wong Education Foundation.

Conflict of interest

The authors declare no conflict of interest.

Keywords: FRET · liposomes · protein–membrane interactions · quenchers · single-molecule studies

How to cite: *Angew. Chem. Int. Ed.* **2019**, *58*, 5577–5581
Angew. Chem. **2019**, *131*, 5633–5637

[1] R. K. Banerjee, A. G. Datta, *Mol. Cell. Biochem.* **1983**, *50*, 3–15.
[2] a) T. S. Ulmer, A. Bax, N. B. Cole, R. L. Nussbaum, *J. Biol. Chem.* **2005**, *280*, 9595–9603; b) C. C. Jao, B. G. Hegde, J. Chen, I. S. Haworth, R. Langen, *Proc. Natl. Acad. Sci. USA* **2008**, *105*, 19666–19671; c) R. Sachl, I. Boldyrev, L. B. A. Johansson, *Phys. Chem. Chem. Phys.* **2010**, *12*, 6027–6034.
[3] a) Y. Li, Z. Qian, L. Ma, S. Hu, D. Nong, C. Xu, F. Ye, Y. Lu, G. Wei, M. Li, *Nat. Commun.* **2016**, *7*, 12906; b) S. Isbaner, N. Karedla, I. Kaminska, D. Ruhlandt, M. Raab, J. Bohlen, A. Chizhik, I. Gregor, P. Tinnefeld, J. Enderlein, R. Tsukanov, *Nano Lett.* **2018**, *18*, 2616–2622; c) C. M. Ajo-Franklin, C. Yoshina-Ishii, S. G. Boxer, *Langmuir* **2005**, *21*, 4976–4983.
[4] a) S. Winterfeld, S. Ernst, M. Borsch, U. Gerken, A. Kuhn, *PLoS One* **2013**, *8*, e59023; b) Y. Haga, K. Ishii, K. Hibino, Y. Sako, Y. Ito, N. Taniguchi, T. Suzuki, *Nat. Commun.* **2012**, *3*, 907.
[5] a) H. Braak, K. Del Tredici, U. Rub, R. A. I. de Vos, E. N. H. J. Steur, E. Braak, *Neurobiol. Aging* **2003**, *24*, 197–211; b) J. Burré, *J. Parkinson Dis.* **2015**, *5*, 699–713.
[6] a) R. B. Gennis, C. R. Cantor, *Biochemistry* **1972**, *11*, 2509–2517; b) J. Lee, S. Lee, K. Ragunathan, C. Joo, T. Ha, S. Hohng, *Angew. Chem. Int. Ed.* **2010**, *49*, 9922–9925; *Angew. Chem.* **2010**, *122*, 10118–10121.
[7] J. W. Taraska, M. C. Puljung, N. B. Olivier, G. E. Flynn, W. N. Zagotta, *Nat. Methods* **2009**, *6*, 532–537.
[8] a) T. Ha, T. Enderle, D. F. Ogletree, D. S. Chemla, P. R. Selvin, S. Weiss, *Proc. Natl. Acad. Sci. USA* **1996**, *93*, 6264–6268; b) C. Joo, S. A. McKinney, M. Nakamura, I. Rasnik, S. Myong, T. Ha, *Cell* **2006**, *126*, 515–527; c) M. Diez, B. Zimmermann, M. Borsch, M. Konig, E. Schweinberger, S. Steigmiller, R. Reuter, S. Felekyan, V. Kudryavtsev, C. A. M. Seidel, P. Graber, *Nat. Struct. Mol. Biol.* **2004**, *11*, 135–141.
[9] S. J. Isak, E. M. Eyring, J. D. Spikes, P. A. Meekins, *J. Photochem. Photobiol. A* **2000**, *134*, 77–85.
[10] B. A. Avelar-Freitas, V. G. Almeida, M. C. Pinto, F. A. Mourao, A. R. Massensini, O. A. Martins-Filho, E. Rocha-Vieira, G. E. Brito-Melo, *Braz. J. Med. Biol. Res.* **2014**, *47*, 307–315.
[11] G. K. Srivastava, R. Reinoso, A. K. Singh, I. Fernandez-Bueno, D. Hileeto, M. Martino, M. T. Garcia-Gutierrez, J. M. Merino, N. F. Alonso, A. Corell, J. C. Pastor, *Exp. Eye Res.* **2011**, *93*, 956–962.
[12] J. S. Gale, A. A. Proulx, J. R. Gonder, A. J. Mao, C. M. L. Hutnik, *Am. J. Ophthalmol.* **2004**, *138*, 64–69.
[13] a) P. Karam, A. T. Ngo, I. Rouiller, G. Cosa, *Proc. Natl. Acad. Sci. USA* **2010**, *107*, 17480–17485; b) E. Rhoades, M. Cohen, B. Schuler, G. Haran, *J. Am. Chem. Soc.* **2004**, *126*, 14686–14687.
[14] J. F. Nagle, S. Tristram-Nagle, *Biochim. Biophys. Acta Rev. Biomembr.* **2000**, *1469*, 159–195.
[15] S. J. Singer, *Annu. Rev. Cell Biol.* **1990**, *6*, 247–296.
[16] G. Stengel, R. Zahn, F. Hook, *J. Am. Chem. Soc.* **2007**, *129*, 9584–9585.
[17] W. Kaiser, U. Rant, *J. Am. Chem. Soc.* **2010**, *132*, 7935–7945.
[18] a) J. Burré, M. Sharma, T. C. Sudhof, *Proc. Natl. Acad. Sci. USA* **2014**, *111*, E4274–E4283; b) G. Fusco, T. Pape, A. D. Stephens, P. Mahou, A. R. Costa, C. F. Kaminski, G. S. K. Schierle, M. Vendruscolo, G. Veglia, C. M. Dobson, A. De Simone, *Nat. Commun.* **2016**, *7*, 12563.
[19] a) C. Wang, C. Zhao, D. Li, Z. Tian, Y. Lai, J. Diao, C. Liu, *Front. Mol. Neurosci.* **2016**, *9*, 48; b) S. B. Lokappa, T. S. Ulmer, *J. Biol. Chem.* **2011**, *286*, 21450–21457.
[20] a) C. M. Pfefferkorn, F. Heinrich, A. J. Sodt, A. S. Maltsev, R. W. Pastor, J. C. Lee, *Biophys. J.* **2012**, *102*, 613–621; b) Z. Jiang, S. K. Hess, F. Heinrich, J. C. Lee, *J. Phys. Chem. B* **2015**, *119*, 4812–4823; c) E. Hellstrand, M. Grey, M. L. Ainalem, J. Ankner, V. T. Forsyth, G. Fragneto, M. Haertlein, M. T. Dauvergne, H. Nilsson, P. Brundin, S. Linse, T. Nylander, E. Sparr, *ACS Chem. Neurosci.* **2013**, *4*, 1339–1351.

[21] a) M. S. Nielsen, H. Vorum, E. Lindersson, P. H. Jensen, *J. Biol. Chem.* **2001**, *276*, 22680 – 22684; b) S. L. Leong, R. Cappai, K. J. Barnham, C. L. Pham, *Neurochem. Res.* **2009**, *34*, 1838 – 1846; c) J. Lautenschläger, A. D. Stephens, G. Fusco, F. Strohl, N. Curry, M. Zacharopoulou, C. H. Michel, R. Laine, N. Nespovitaya, M. Fantham, D. Pinotsi, W. Zago, P. Fraser, A. Tandon, P. St George-Hyslop, E. Rees, J. J. Phillips, A. De Simone, C. F. Kaminski, G. S. K. Schierle, *Nat. Commun.* **2018**, *9*, 712.

[22] S. Tamamizu-Kato, M. G. Kosaraju, H. Kato, V. Raussens, J. M. Ruysschaert, V. Narayanaswami, *Biochemistry* **2006**, *45*, 10947 – 10956.

[23] Z. T. Zhang, C. Y. Dai, J. Bai, G. H. Xu, M. L. Liu, C. G. Li, *Biochim. Biophys. Acta Biomembr.* **2014**, *1838*, 853 – 858.

[24] a) F. X. Contreras, L. Sanchez-Magraner, A. Alonso, F. M. Goni, *FEBS Lett.* **2010**, *584*, 1779 – 1786; b) V. A. Fadok, D. R. Voelker, P. A. Campbell, J. J. Cohen, D. L. Bratton, P. M. Henson, *J. Immunol.* **1992**, *148*, 2207 – 2216.

[25] N. Yan, *Trends Biochem. Sci.* **2013**, *38*, 151 – 159.

Manuscript received: December 6, 2018
Revised manuscript received: February 11, 2019
Accepted manuscript online: March 6, 2019
Version of record online: March 26, 2019

